NMR Shieldings and Electron Correlation Reveal Remarkable Behavior on the Part of the Flavin N_5 Reactive Center

Joseph D. Walsh[†] **and Anne-Frances Miller***[,‡]

Departments of Biophysics and Chemistry, The Johns Hopkins University, Baltimore, Maryland 21218, and Department of Chemistry, The University of Kentucky, Lexington, Kentucky 40506

Received: September 5, 2002; In Final Form: September 17, 2002

NMR calculations on oxidized lumiflavin using density functional theory (DFT) reveal that methods including electron correlation show significant improvements in the flavin carbon and nitrogen NMR shieldings over uncorrelated Hartree−Fock (HF) results. In particular, the GIAO B3PW91//B3PW91 cc-pVTZ NMR shielding of the important N_5 reactive center shows an improvement of 60.7 ppm over GIAO HF//B3PW91 cc-pVTZ, bringing it to within 6.1 ppm of the solvent-corrected experimental value. While the N_5 center becomes dramatically shielded upon going from HF to correlated NMR shieldings, with the exception of C_{10a}, all other NMR resonances are systematically *deshielded*. The nitrogens N_1, N_3, and N_{10} become deshielded by 23−26 ppm, and carbons become deshielded by an average of 5.2 ppm, bringing them into better agreement with experiment. Similar results are obtained with the significantly smaller 6-311G(d,p) basis set. The effects of electron correlation through the flavin geometry are also evident. The geometries calculated by B3LYP, B3PW91, and MP2 correlated methods using the 6-311G(d,p) basis lead to systematic NMR deshielding for *all* flavin heavy atoms in comparison with those obtained at the HF geometry. On average, the flavin nitrogens become deshielded by more than 10 ppm and carbons by almost 4 ppm. Similar changes, but of smaller magnitude, are observed for the NMR shieldings of fully reduced flavin, indicating that electron correlation is less important in that flavin state. The magnitude of the dramatic NMR shielding increase of several electrophilic centers upon flavin reduction is well captured by DFT methods. In particular, the GIAO B3PW91/cc-pVTZ N_5 NMR shielding difference between oxidized and reduced flavin is 299.6 ppm, which compares well to the solvent-corrected experimental shielding difference of 299.1 ppm. The N_5 center is also remarkable for its large decrease in shielding, by 33.4 ppm (98.0 ppm deshielding of σ_{11}), upon protonation of the oxidized flavin at N_1, a process which activates N_5 for electrophilic attack.

Flavins (7,8-dimethyl-10-alkylisoalloxazines, Figure 1) catalyze a wide variety of reactions because of tuning of their reduction potentials by the flavoenzymes that bind them. These reactions range from oxidations and dehydrogenations to hydroxylations and electron-transfer processes. Flavoproteins have been classified upon the basis of their biological function, stabilization of the flavin semiquinone, and the reactivity of the oxidized and reduced flavins toward sulfite and oxygen, respectively. These classifications based on reactivity also correlate to some degree with structural motifs, such as the presence or absence of a basic protein side chain near N_1, hydrogen bonding at N_5, and the flavin "butterfly" bend angle.[1−4] For instance, the reduced flavoenzyme oxidases of D-amino acids, glucose, cholesterol, and others are readily reoxidized upon exposure to molecular oxygen without formation of intermediates. They stabilize the red anionic semiquinone intermediate upon one-electron reduction. Oxygenases, in contrast, once reduced, react with O_2 to form a C_{4a} peroxyflavin intermediate allowing for the hydroxylation of substrate and formation of a C_{4a} hydroxyflavin. The dehydrogenase/flavin electron transferase class however reacts very slowly with O_2, resulting in superoxide and flavin semiquinone, which is thermodynamically stabilized. Examples include acyl-CoA dehydrogenase and flavodoxins.

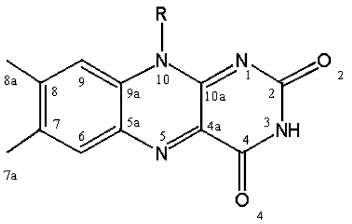

Lumiflavin:
R = CH_3

FMN:
R = $CH_2(CHOH)_3CH_2OH_2PO_3$

FAD:
R = $CH_2(CHOH)_3CH_2O(HPO_3)_2$ -adenosine

Figure 1. Computations presented in this work were performed on lumiflavin, which shares the reactivity of the biological cofactors flavin mononucleotide (FMN) and flavin adenine dinucleotide (FAD). The planar oxidized state is depicted, which upon two-electron reduction becomes protonated at N_5 and N_1 and acquires a butterfly bend about the N_5-N_{10} axis.

In oxidized flavoproteins, it is the N_5 site that reacts with reduced pyridine nucleotides and both N_5 and C_{4a} react with sulfite, depending upon the activation of the sites, as well as steric factors.[5−8] However, while C_{4a} and N_5 are the most electrophilic sites, other reactive centers exist. This is evidenced

[†] The Johns Hopkins University.
[‡] The University of Kentucky.

10.1021/jp022005j CCC: $25.00
Published on Web 12/31/2002

by C_{10a} peroxyflavin adducts and naturally occuring covalent modifications of flavins and flavins covalently bound to protein at the C_6 and C_8 positions.[9]

The interactions of flavoproteins with the flavin cofactor probably have such a powerful effect on the reactivity and redox potentials because of the very highly delocalized nature of the flavin ring system.[10] This means that electron correlation is expected to play a large role in flavin redox properties. Many calculations have been carried out on flavins and even flavin−flavoprotein active site models,[11−14] yet most of these have not used geometries optimized by correlated methods.[11,15−23] In those flavin studies of which we are aware[24−26] that have used correlated flavin properties and geometries, in only one case was the effect of correlation addressed explicitly.[26]

In this work, we present the first NMR shielding calculations on the flavin redox cofactor, showing the significance of electron correlation on oxidized and reduced flavins via the effect on NMR shieldings of important flavin redox centers, in particular, N_5. We also present the effects that electron correlation has on NMR shieldings indirectly through the effect of correlation on the flavin geometry.

The flavin NMR shieldings show a large variation between different flavoenzymes.[27] Indeed, we observe that data of Müller et al. show that for *every* carbon and nitrogen resonance on the flavin, the *range* of shielding values observed in flavoenzymes is larger than the shielding difference between flavin in chloroform and in aqueous solution (this is true for both oxidized and fully reduced flavins).[28] Hence, flavoenzymes are apparently more effective at polarizing the flavin molecule than is aqueous solution. Given the importance of these polarizing interactions in this highly delocalized molecule, it is imperative to address electron correlation effects.

Massey and Hemmerich proposed that flavoenzyme reactivity is controlled by electrostatic interactions, hydrogen bonding, and bending of the flavin.[1] Numerous subsequent model studies that measured reactivity and redox potentials as a function of hydrogen bond formation and conformational distortion of the flavin have supported their basic postulates.[4,7,8,29−34] Further, attempts have been made to correlate the N_5 and N_1 NMR shieldings in flavoenzymes with strength of hydrogen bonding between protein and flavin at those positions.[35]

Attention to the flavin butterfly bend is important because this affects the pyramidalization angles of both N_5 and N_{10}. Hence, suggestions that the reduced flavin butterfly bend angle may be related to the flavin reactivity, because different classes of flavoenzymes appear to display consistently different flavin bend angles, make chemical sense.[1,2,28]

However, relationships between pyramidalization angles and NMR shielding (or reactivity) are neither straightforward nor universal. While correlations are seen for some systems such as bowl-shaped hydrocarbons related to C_{60} and also in C_{70},[36,37] in reduced fullerene systems with many distinct pyramidalization angles and carbon NMR shieldings, such as $C_{60}-H_2$ and $C_{60}-H_6$, such correlations are not seen.[38,39] In the case of flavins, semiempirical interpretations of the experimental carbon NMR shieldings as diagnostic of the flavin bend or, more particularly, the degree of sp^2 vs sp^3 hybridization of the N_5 and N_{10} have been made.[28] In the present work, we present some computational evidence for a relation between pyramidalization angle and N_{10} shielding.

Finally, beyond the application of elucidation of structure, the NMR shielding of different nuclei around the flavin ring system represents a possible probe of the chemical properties of flavin reactive groups, as argued here. One possible approach is to interpret flavin reduction potentials in terms of flavin stability (aromaticity) as determined by nucleotide independent chemical shifts (NICS).[40] However, this method is not directly experimentally verifiable. Also, using the average of many flavin (carbon) resonances would require extensive flavin isotope labeling, and the range of shielding values in flavin carbon (and particular benzene ring) resonances is probably too small for this approach to yield accurate results. In contrast to this, the N_5 nitrogen shows a remarkably large variation (>40 ppm) in resonance among different flavoproteins, making it a prime candidate for investigation of whether NMR shieldings can serve as useful diagnostic tools for flavin reactivity and reduction potentials.

Computational Methods

The computational investigation of flavins is addressed via the lumiflavin molecule. Lumiflavin has a methyl group at the N_{10} position instead of the methylene in 5′-phosphoribose and 5′-phosphoribose AMP of FMN and FAD, respectively (see Figure 1). However, it retains the characteristic flavin reactivity.[5,41] Correlated and uncorrelated methods were compared by way of comparing GIAO NMR shielding results of the B3LYP and B3PW91 hybrid density functionals with Hartree−Fock results.[42−44] The triple-ζ basis sets by Pople, 6-311G(d,p), and Dunning, cc-pVTZ, were used. Although second-order Møller−Plesset (MP2) GIAO NMR calculations were not undertaken, geometry optimizations by MP2 provided comparison to the DFT geometry results. It should be noted that the density functional NMR results are known not to fully capture correlation effects because the functionals presently available have no current dependence.[45,46] The notational convention is used throughout whereby the method used for NMR shielding calculation is separated from that used for the geometry optimization by a double-slash. All computations were done using the Gaussian 98 package, revisions 6−9, and run on the X- and N-class HP supercomputers.[47]

The experimental chemical shifts were taken from values published by Müller et al. for oxidized tetraacetylriboflavin (TARF) and fully reduced $TARFH_2$ in chloroform at 299 ± 2 K.[28] These experimental chemical shifts are converted to chemical *shieldings* with the aid of the known absolute shieldings of nuclei in reference molecules. In the case of nitrogen, the ammonia reference with an experimental gaseous chemical shielding of 264.5 ppm is adjusted to 244.6 ppm by adding the gas to liquid resonance shift.[48] The negative of the experimental flavin nitrogen shifts (relative to liquid ammonia) are then added to the absolute shielding of the liquid ammonia reference. The carbon shifts are converted in a similar manner to shieldings by using the TMS reference compound carbon shielding of 188.1 ppm, adjusted with the gas to liquid resonance shift to 186.4 ppm. In this later case, it should be noted that this is the neat liquid TMS value, while the experimental reference value comes from TMS solute in chloroform. The NMR reference values refer to measurements made at 300 K.[49,50]

The computations refer to in vacuo flavin molecules, unpolarized by any solvent molecules, whereas the NMR shift measurements were made in chloroform. While chloroform is often thought of as a nonpolar and fairly innocuous solvent, its polarization effect on nitrogen NMR shieldings can be substantial. The NMR shift of the pyridine nitrogen in chloroform is shielded by 12.5 ± 1.5 ppm with respect to vacuum measurements.[51] Because chloroform may only donate hydrogen bonds and not accept them, it directly effects mainly the pyridine-type nitrogens N_1 and N_5 of the oxidized flavin molecule. Hence,

TABLE 1: The Calculated Oxidized Lumiflavin Bond Lengths Using the 6-311G(d,p) Basis Set

	oxidized lumiflavin bong lengths, Å				
bond	HF	MP2	B3LYP	B3PW91	exptl[a]
C_2-O_2	1.184	1.213	1.210	1.209	1.221
C_2-N_3	1.398	1.416	1.416	1.411	1.394
N_3-C_4	1.364	1.379	1.380	1.376	1.352
C_4-O_4	1.183	1.214	1.210	1.208	1.212
C_4-C_{4a}	1.499	1.504	1.501	1.496	1.506
$C_{4a}-C_{10a}$	1.470	1.462	1.462	1.457	1.447
$C_{10a}-N_1$	1.281	1.308	1.302	1.300	1.309
N_1-C_2	1.375	1.388	1.383	1.379	1.366
$C_{10a}-N_{10}$	1.357	1.379	1.384	1.379	1.371
$N_{10}-C_{11}$	1.464	1.465	1.468	1.460	1.475
$C_{4a}-N_5$	1.263	1.306	1.295	1.293	1.296
N_5-C_{5a}	1.372	1.373	1.368	1.364	1.378
$N_{10}-C_{9a}$	1.387	1.384	1.386	1.381	1.375
$C_{5a}-C_6$	1.398	1.409	1.407	1.405	1.391
$C_{9a}-C_9$	1.398	1.409	1.403	1.400	1.410
C_9-C_8	1.379	1.393	1.390	1.388	1.378
C_8-C_7	1.413	1.423	1.422	1.420	1.425
C_6-C_7	1.370	1.388	1.381	1.379	1.378
C_8-C_{8a}	1.509	1.507	1.507	1.501	1.506
C_7-C_{7a}	1.510	1.507	1.508	1.502	1.492
$C_{5a}-C_{9a}$	1.391	1.418	1.416	1.414	1.401

[a] The experimental bond lengths are from the structure of Tanaka et al.[58]

solvent-corrected shielding values (adjusted by −12.5 ppm) for these nitrogens are quoted in parentheses where appropriate, while all other nitrogen and carbon resonances are left uncorrected. Also, unless explicitly stated the uncorrected values are used in the figures and tables.

Results and Discussion

Oxidized Lumiflavin: NMR and Electron Correlation. The geometries of oxidized flavin derivatives have been characterized by numerous X-ray crystal structures.[52−57] Comparison with theory is difficult, however, because the uncertainties in bond lengths for the best of the experimental structures are not much better than 0.02 Å. Also, different flavin derivatives result in different crystal packing forces on the flavin, which yield a range of bond lengths, especially on the uracil end of the flavin. Nonetheless, comparison of calculated with experimental geometries does reveal one significant insight. The calculated HF bond lengths are shorter than the experimental bounds of error for the two flavin carbonyl groups, and more significantly, the catalytically important N_5-C_{4a} and $C_{10a}-N_1$ bonds are too short by 0.033 and 0.028 Å, respectively (see Table 1). Hence, the HF level of description of the flavin fails in this regard in comparison to experiment. Both hybrid DFT methods and MP2 are in good agreement with experiment. Further refinements in the theoretical description, such as basis set expansion or use of different correlation functionals, does not add any further insight because these modifications lead to results all lying within the bounds of the experimental structure uncertainty. However, while direct comparison with geometry is not useful for refinement of the description of flavins, the effect electron correlation has on NMR shieldings, directly and also indirectly through the geometry, *does* prove to be a useful measure.

The carbon and nitrogen NMR shieldings calculated with HF, B3LYP, and B3PW91 GIAO methods for HF-, B3LYP-, B3PW91-, and MP2-optimized geometries are presented in Table 2. The 6-311G(d,p) basis set was used so that flavin geometry optimizations could be performed at the MP2 level and compared with the other methods. While electron correlation has an effect on NMR shieldings through its effect on the flavin geometry, the generaly larger effect is due to correlation incorporated directly in the flavin electronic wave function/density in the GIAO NMR calculation, and hence we discuss this first.

Comparison of carbon NMR shieldings obtained by DFT methods with HF results shows consistent deshielding of the resonances. The two functionals used however themselves show

TABLE 2: The GIAO NMR Shieldings of Nitrogens and Carbons of the Neutral Oxidized Lumiflavin Molecule[a]

	oxidized lumiflavin nitrogen and carbon absolute NMR shieldings, ppm											
	HF//HF	HF//D_1	HF//D_2	HF//MP2	D_1//HF	D_1//D_1	D_1//MP2	D_2//HF	D_2//D_2	D_2//MP2	D_2//D_2 cc-pVTZ	exptl
						Carbons						
C_{10a}	37.2	31.9	32.9	31.4	35.6	31.0	30.6	39.8	36.4	35.0	35.1	35.9
C_2	42.2	35.6	36.2	34.6	34.6	29.1	28.2	38.3	33.6	32.2	31.1	29.8
C_4	37.6	30.1	30.7	29.2	30.1	24.0	23.3	33.7	28.5	27.3	25.8	25.2
C_{4a}	57.2	53.0	53.8	49.9	44.6	41.4	38.9	48.1	46.0	42.7	44.0	49.4
C_{5a}	64.1	59.6	60.4	57.5	49.0	44.6	42.6	53.2	49.6	47.0	48.8	50.4
C_6	53.7	50.5	50.8	49.6	46.1	42.7	43.6	49.8	47.7	46.5	47.7	52.2
C_7	60.2	58.5	59.1	56.9	45.3	41.7	43.1	49.4	48.1	46.0	48.1	48.4
C_{7a}	176.5	175.3	175.4	174.8	164.1	162.1	162.6	167.1	165.7	165.1	165.5	165.6
C_8	40.9	36.6	37.0	35.9	33.7	30.0	30.6	38.0	35.7	34.4	35.6	37.5
C_{8a}	174.1	172.9	172.9	172.6	161.6	160.3	159.9	164.6	163.3	162.9	163.2	163.6
C_9	80.0	78.6	79.1	77.6	67.5	65.6	64.8	70.7	69.3	68.1	69.2	69.5
C_{9a}	56.2	51.8	52.8	51.8	49.6	45.9	45.7	53.9	51.5	50.3	51.0	53.8
Δ	8.2	4.4	5.0	3.4	−1.6	−5.0	−5.9	2.1	−0.5	−2.0	−1.4	
R	12.4	14.1	13.7	13.7	11.0	7.9	8.9	11.0	8.4	9.1	6.7	
σ	4.7	5.3	5.2	5.1	3.4	2.6	2.9	3.4	2.4	2.8	2.0	
						Nitrogens						
N_1	59.8	53.3	53.6	55.8	32.6	25.2	25.0	37.4	32.8	30.1	33.1	44.5 (32.0)
N_3	116.0	107.7	109.0	107.7	86.9	77.6	77.7	89.9	82.1	81.0	81.9	85.0
N_5	−158.7	−184.7	−182.8	−189.6	−116.6	−129.5	−131.7	−110.8	−121.4	−125.2	−120.0	−101.4 (−113.9)
N_{10}	136.5	124.4	125.6	122.6	106.6	95.9	94.9	109.3	100.3	97.8	100.9	92.7

[a] The B3LYP and B3PW91 hybrid functionals are indicated by D_1 and D_2, respectively. The basis set was 6-311G(d,p), except where indicated. The experimental nitrogen shifts are taken from data of Müller et al.[28] and adjusted to experimental shieldings as discussed in the Computational Methods section. The N_5 and N_{10} experimental shielding values corrected for solvent hydrogen bonding are given in parentheses. Some features of the carbon shieldings are summarized in the Δ, R, and σ values. These represent the mean difference between the calculated and experimental carbon shieldings and the range and standard deviation in values about that mean, respectively.

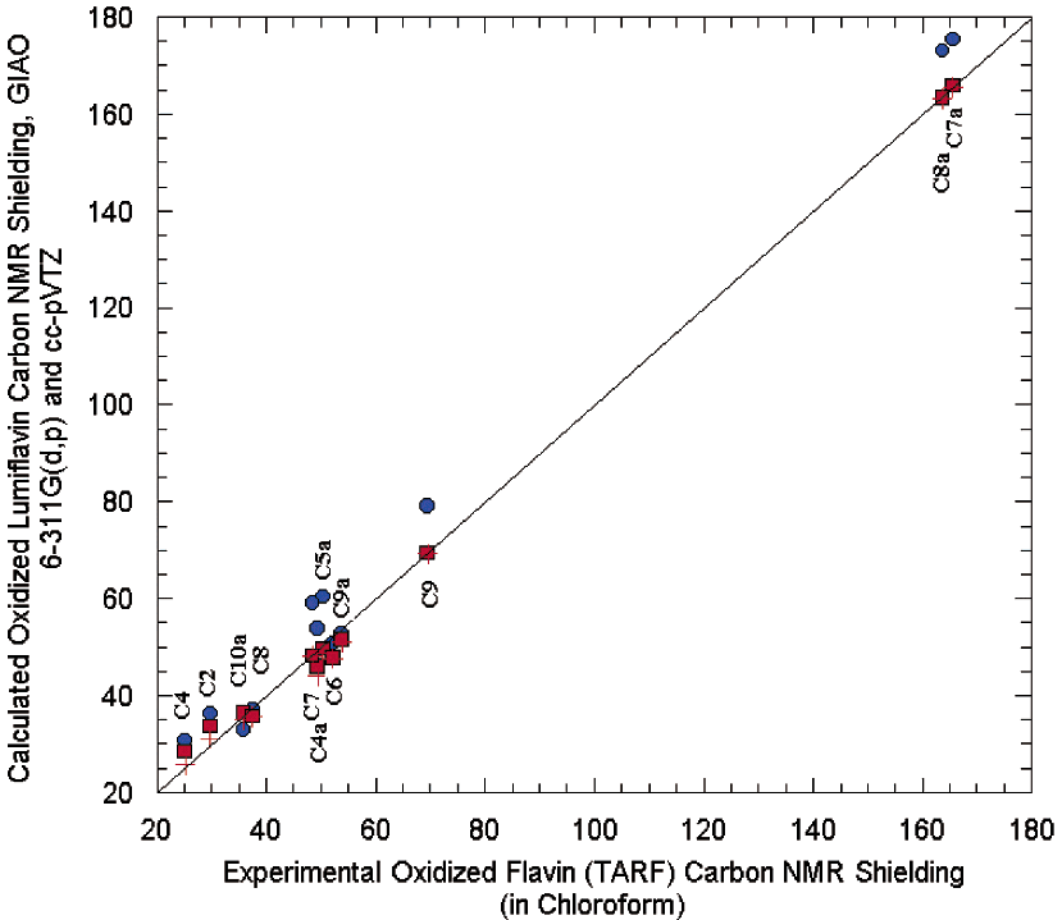

Figure 2. Calculated oxidized lumiflavin vs experimental oxidized tetraacetylriboflavin (TARF) carbon NMR shieldings. Comparison of shielding results without and with electron correlation is shown: (blue ●) the 6-311G(d,p) HF//B3PW91 and (red ■) 6-311G(d,p) B3PW91//B3PW91. The latter agree well with (red +) the cc-pVTZ B3PW91//B3PW91 results.

a considerable difference in the degree of deshielding. On average, the B3PW91 GIAO results are deshielded by 5.5 ppm in comparison with the HF GIAO results, whereas the B3LYP GIAO results show a deshielding by an average of 9.3 ppm by comparison with HF GIAO. The average referred to here is across all carbon nuclei, comparing the DFT GIAO results with the HF GIAO results obtained for a given geometry (HF, DFT, MP2). The deshielding resulting from the B3LYP functional indeed appears to be excessive. Table 2 shows that in the cases of B3LYP and MP2 geometries the B3LYP carbon resonances are (in the mean) too deshielded by 5 and 5.9 ppm in comparison with experiment (of course the HF results are too shielded by almost this amount). In contrast with this, the B3PW91 carbon shieldings are only about 0.5−2 ppm too deshielded (depending on the geometry). In fact, the B3PW91//B3PW91 6-311G(d,p) carbon shielding results compare favorably to all others, including even the B3PW91//B3PW91 cc-pVTZ results, and are shown in Figure 2, along with the HF//B3PW91 carbon shieldings. From this figure, it is obvious that both the scatter and the mean offset from experiment of carbon resonances are improved by electron-correlated methods.

For the nitrogens N_1, N_3, and N_{10}, the effect of correlation on shielding is much greater than for the carbons. For instance, comparison of B3PW91//B3PW91 with HF//B3PW91 shows a deshielding of 23−26 ppm, and comparison of B3LYP//B3LYP with HF//B3LYP shows a deshielding of 28−30 ppm. Again the effect of the B3LYP functional is greater, although, unlike the case of the carbon shieldings, it is not possible to conclude that the B3LYP functional results in overly deshielded resonances.

The N_5 nitrogen represents a uniquely interesting case. Unlike all others, the N_5 nucleus actually becomes more *shielded* in going from HF to DFT NMR results. The B3LYP//B3LYP and B3PW91//B3PW91 N_5 NMR shieldings are 55.2 and 61.4 ppm, respectively, more shielded than the HF//B3LYP and HF//B3PW91 results. Again, the B3PW91 functional appears to perform somewhat better than B3LYP. The improvements obtained by use of the larger cc-pVTZ (738 functions) basis set over the 6-311G(d,p) basis set (414 functions) are only minor with deviation of the N_5 shielding from the solvent-corrected experimental value improving from 7.5 to 6.1 ppm. The B3PW91 and HF nitrogen shielding results are shown in Figure 3.

Although the two density functionals used both agree quite well, the B3PW91 functional leads consistently to slightly more shielded nitrogen NMR than B3LYP. A possible trend is seen, as (for both HF and MP2 geometries) the difference between these two functionals consistently increases with degree of deshielding of the nitrogen: from 3 ppm for the most shielded nitrogen, N_{10}, to roughly 6 ppm for the most deshielded nitrogen, N_5.

Electron correlation also indirectly affects the carbon and nitrogen NMR shieldings through the geometry. The mean NMR shieldings of carbons become more deshielded by almost 4 ppm because of inclusion of correlation effects in geometry optimization. This is likely due to the slight but consistent increases in bond lengths for the DFT and, in particular, MP2 geometries by comparison with HF (see Table 1).[59−61] Levels of deshielding increase in the order of the geometries HF, B3PW91, B3LYP, and MP2. However, the comparison of nitrogen shieldings

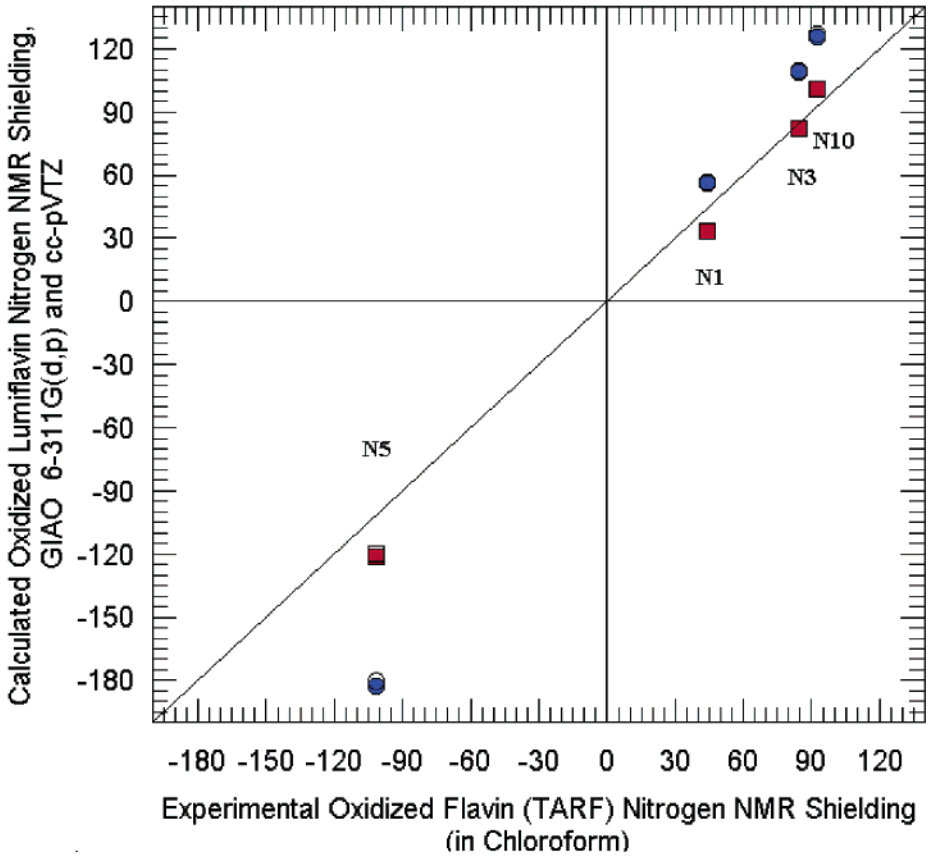

Figure 3. Calculated oxidized lumiflavin vs experimental oxidized tetraacetylriboflavin (TARF) nitrogen NMR shieldings. The oxidized lumiflavin nitrogen shieldings with and without electron correlation were calculated with the 6-311G(d,p) basis set, (blue ●) HF//B3PW91, (red ■) B3PW91//B3PW91. The corresponding cc-pVTZ shieldings are (open ○) HF//B3PW91, and (open □) B3PW91//B3PW91.

obtained with DFT and MP2 geometries indicates that there is no substantial difference on account of the slightly differing geometries obtained by these methods. As is the case for nitrogen, the carbon B3LYP and B3PW91 NMR shieldings calculated with the B3LYP and B3PW91 geometries agree well with the B3LYP and B3PW91 shieldings calculated at the MP2 geometries. The agreement is well within 1.5 ppm for most shieldings, except notably for the carbons flanking the N_5 center, C_{5a} and C_{4a}, where the differences are 2−3 ppm. These results once again indicate that geometrical electron-correlation effects are captured by hybrid DFT methods as well as they are by MP2 and that again the N_5 part of the molecule stands out as the most difficult to predict. The greater importance of electron correlation directly vs indirectly through the geometry on the NMR shieldings is made clearer in Figure 4 for the four flavin nitrogens. The N_1 and N_5 shieldings have not been adjusted for the increased shielding caused by the chloroform solvent.

Reduced Lumiflavin: NMR and Electron Correlation. Small molecule crystal structures of reduced flavin derivatives present more problems than their oxidized counterparts. For the oxidized flavin structures, the substituents were generally distant from the catalytically important $N_5{=}C_{4a}{-}C_{10a}{=}N_1$ diazabutadiene moiety. Furthermore, the oxidized flavin is planar, so crystal structures that show significant deviations from planarity can be discarded from consideration of comparison with theory. The fully reduced flavin however is bent about the $N_5{-}N_{10}$ axis, although the exact amount of the butterfly bend angle is uncertain because different flavin derivatives show different bend angles. Furthermore, substituents (alkylations) are generally found on the N_1 and most problematically on the N_5 position.[62−65] This makes these derivatives chemically distinct from the biologically relevant flavins FMN, FAD, and lumiflavin.

One prominent exception is the crystal structure of the N_{10}-propyl-linked flavin−nicotinamide biscoenzyme of Porter and Voet, which is not substituted in any position on the isoalloxazine rings.[66] However, even in this case, the butterfly bend has probably been influenced by crystal structure packing forces, as noted by the authors. This will no doubt change other geometrical parameters such as bond lengths and angles related to the N_5 and N_{10} centers. Hence, any comparison between experimental reduced flavin crystal structure and calculated geometries is intrinsically problematic and is not undertaken here.

The flavin B3LYP and B3PW91 GIAO NMR shieldings calculated with the 6-311G(d,p) basis set at the HF, B3LYP, B3PW91, and MP2 geometries are shown in Table 3. Many of the observations made for the oxidized flavin also hold true for the reduced state. Once again, the DFT carbon and nitrogen resonances are deshielded with respect to the HF ones. Again, the B3LYP results in the greatest deshielding, giving, for instance, B3LYP//B3LYP mean carbon shieldings 4.3 ppm less than the experimental mean value. The B3PW91 functional again appears to represent a halfway point between the too-shielded HF GIAO and too-deshielded B3LYP GIAO results. The B3PW91//B3PW91 mean carbon shielding is only 0.3 ppm more shielded than the experimental mean. Again the agreement with the larger cc-pVTZ basis set is good. Notably, for the reduced flavin, the nitrogen shieldings *all* become more deshielded in going from HF GIAO to DFT GIAO results (Figure 5). The N_5 resonance has moved considerably upfield, and this means that the reduced flavin nitrogen shielding range is only $^1/_3$ of the range in the oxidized state.

The effect of electron correlation on NMR shieldings through the geometry is slightly smaller than was observed for the

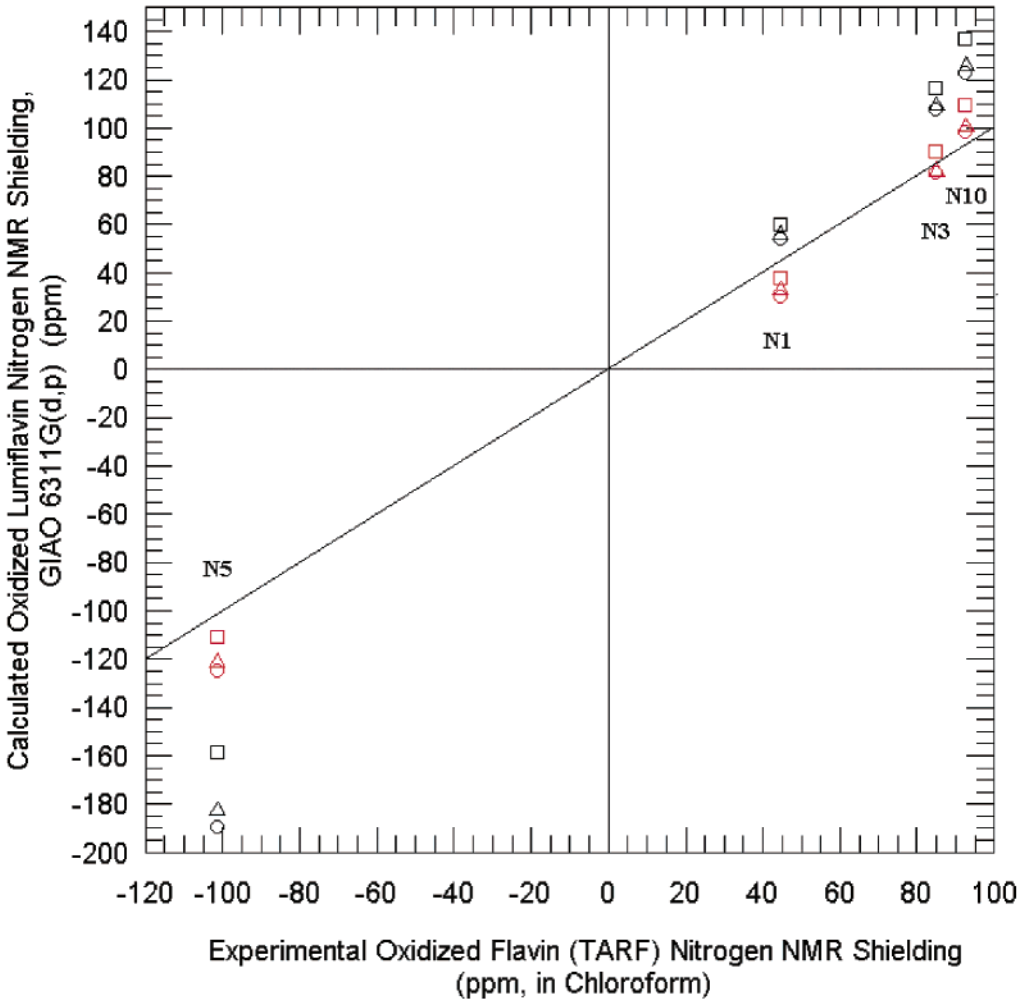

Figure 4. The combined effects of electron correlation (in the geometry and in the shielding calculation) on the NMR shieldings for the nitrogens of oxidized flavin. The results compared are as follows: (black □) HF//HF; (black △) HF//B3PW91; (black ○) HF//MP2; (red □) B3PW91//HF; (red △) B3PW91//B3PW91; (red ○) B3PW91//MP2.

oxidized state. While this difference is generally <1 ppm for the mean carbon shieldings, it can be several ppm for the nitrogens. This suggests that electron correlation is less significant in determining the reduced-state geometry than the oxidized-state geometry.

The optimized geometries of 1,5-dihydrolumiflavin obtained by HF, DFT, and MP2 methods differ most obviously in their differing flavin butterfly bends. The dihedral and pyramidalization angles for the central nitrogens N_5 and N_{10} are shown in Table 4. Interestingly, the DFT dihedral angles differ by less than 3° from those of the HF geometry, the latter being more bent. The MP2 geometry however is roughly 10° more bent than that from DFT results (B3LYP and B3PW91 give equivalent results). Despite these large geometrical differences, the N_1 and N_3 shieldings of DFT and MP2 geometries are essentially identical, and the shieldings calculated using the HF geometry differ from these by 6−8 ppm. Furthermore, N_5 and N_{10} NMR shieldings appear to be not at all diagnostic of the flavin dihedral bend angle (see Figure 5 and Table 5). For these two nitrogens, the order in decreasing shielding is HF, DFT, MP2, while the order of increasing butterfly bend angle was DFT, HF, MP2.

While the butterfly bend of the flavin makes the most dramatic impression, it is not the parameter that is most relevant for the N_5 and N_{10} centers; it may vary over a large range without necessarily much affecting the pyramidalization angles (hybridization) of N_5 and N_{10}. Torsional angles are known not to be the best measure of molecular properties (such as π-orbital overlap); a far better measure is the pyramidalization angle of the conjugated center.[67] The pyramidalization is quantified by the use of the π-orbital axis vector (POAV), which makes equal angles, $\Theta_{\sigma\pi}$, with the three σ-bonds.[68,69] This angle varies from 90° for an sp^2 hybridized center to 109.47° for sp^3 hybridization, and beyond. The pyramidalization angles of N_5 and N_{10}, defined as $\Theta_P = (\Theta_{\sigma\pi} - 90)°$ are quoted in Table 4.

The N_{10} pyramidalization angles of HF, DFT, and MP geometries become successively greater with a concomitant shielding decrease (this is true of both HF and DFT NMR shieldings). The N_5 pyramidalization angle of the HF geometry is more similar to MP2 than DFT is, so there is no relation between this angle and the N_5 shielding. Hence, it appears that the nitrogen shieldings of these important centers cannot be simply attributed to the local degree of sp^2 hybridization (π-orbital density) as previously proposed, but, possibly because of the nonlocal component of NMR shieldings,[70−72] appear much more related to electron correlation in the molecule as a whole.

Reactivity and NMR Shieldings. Comparison of different redox states of the flavin requires the use of correlated methods because the number of electrons differs between these states. Hence, we consider here only the density functional NMR

TABLE 3: The GIAO NMR Shieldings of Nitrogens and Carbons of the Neutral Fully Reduced Lumiflavin Molecule[a]

	reduced lumiflavin nitrogen and carbon NMR shieldings, ppm											
	HF//HF	HF//D_1	HF//D_2	HF//MP2	D_1//HF	D_1//D_1	D_1//MP2	D_2//HF	D_2//D_2	D_2//MP2	D_2//D_2 cc-pVTZ	exptl
						Carbons						
C_{10a}	49.3	44.8	45.7	42.4	45.4	41.8	40.0	49.6	47.1	44.3	46.3	47.9
C_2	43.9	38.2	39.0	37.1	39.6	35.0	33.9	43.4	39.9	38.0	37.9	34.4
C_4	34.2	28.0	28.8	27.3	31.6	27.2	26.3	35.6	32.2	30.5	30.1	28.0
C_{4a}	99.0	96.5	97.3	92.9	80.9	78.0	75.3	84.5	82.6	79.2	82.5	79.8
C_{5a}	50.7	48.7	49.4	46.8	41.1	39.7	37.8	45.6	45.0	42.6	44.6	49.0
C_6	75.1	73.8	74.3	70.9	67.1	65.7	63.2	70.5	69.6	66.8	69.1	68.9
C_7	55.4	52.5	53.2	52.1	46.5	43.9	43.4	50.7	49.0	47.9	48.3	51.4
C_{7a}	176.0	174.8	174.9	174.5	163.8	162.5	162.0	166.8	165.6	165.1	165.5	166.1
C_8	62.8	61.2	61.9	58.0	52.0	50.3	47.5	56.2	55.4	51.9	54.5	56.0
C_{8a}	176.1	174.9	175.0	174.3	163.7	162.3	161.7	166.8	165.5	164.7	165.7	166.1
C_9	73.6	71.9	72.4	72.0	67.3	65.9	65.8	70.8	69.9	69.4	69.7	67.0
C_{9a}	61.3	59.7	60.6	56.1	49.7	47.9	45.3	54.0	53.2	49.9	53.0	56.8
Δ	7.2	4.5	5.1	2.7	−1.9	−4.3	−5.8	1.9	0.3	−1.8	−0.3	
R	17.7	19.8	19.7	18.6	13.2	9.9	10.9	12.5	9.5	10.5	7.9	
σ	4.7	5.2	5.1	5.2	4.0	3.2	3.7	3.8	3.0	3.4	2.7	
						Nitrogens						
N_1	159.9	151.3	152.4	151.2	135.9	127.2	127.0	138.6	131.4	130.0	131.4	124.7
N_3	124.5	116.9	118.3	115.7	99.5	91.9	90.3	102.6	96.6	93.6	96.0	95.6
N_5	217.8	214.6	215.6	210.6	181.9	177.3	174.3	184.9	181.4	177.6	179.6	185.2
N_{10}	208.4	201.8	203.6	196.7	174.6	168.0	163.5	177.1	172.6	166.4	171.0	167.8

[a] The B3LYP and B3PW91 hybrid functionals are indicated by D_1 and D_2, respectively. The basis set was 6-311G(d,p), except where indicated. The experimental nitrogen shifts are taken from data of Müller et al.[28] and adjusted to experimental shieldings as discussed in the Computational Methods section. Some features of the carbon shieldings are summarized in the Δ, R, and σ values. These represent the mean difference between the calculated and experimental carbon shieldings and the range and standard deviation in values about that mean, respectively.

TABLE 4: The N_5 and N_{10} Pyramidalization Angles (Θ_P), Dihedral Angles, and Isotropic NMR Shieldings (σ_{iso}) of Neutral Reduced Lumiflavin from Structures Optimized by HF, B3PW91, B3LYP, and MP2 Methods and the 6-311G(d,p) Basis Set[a]

	The Lf_{rd} N_5 and N_{10} pyramidalization and dihedral angles (deg) and GIAO NMR nitrogen shielding (ppm)			
NMR/geometry	HF	B3LYP	B3PW91	MP2
Θ_P N_5	13.0	11.2	11.3	14.6
σ_{iso} N_5 B3PW91	184.9		181.4	177.6
σ_{iso} N_5 B3LYP	181.9	177.3		174.3
Θ_P N_{10}	1.4	3.3	3.4	9.3
σ_{iso} N_{10} B3PW91	177.1		172.6	166.4
σ_{iso} N_{10} B3LYP	174.6	168.0		163.5
	Dihedral Angle			
$C_{10a}N_{10}N_5C_{5a}$	−151.9	−154.2	−155.0	−142.6
$C_{4a}N_5N_{10}C_{9a}$	150.6	153.0	152.8	142.8

[a] Both N_5 and N_{10} nuclei become successively less shielded in the order of geometries HF > DFT > MP2 presented in the table; however, only the N_{10} pyramidalization angle increases in this order.

shieldings, using geometries obtained with the same correlated methods.

It is notable that the reduced minus oxidized difference between B3PW91/cc-pVTZ NMR shieldings shows dramatic increases in shieldings for several particular centers, while all others show only small changes. These results are in good agreement with experimental values, and we especially note here that the centers with large shielding changes correlate with reactive sites.

For instance, the N_5 shielding changes by an impressive 299.6 ppm (expt 299.1 ppm), whereas the other nitrogens show much smaller changes, 98.3 ppm (expt 92.7 ppm) for N_1, 70.1 ppm (expt 75.1 ppm) for N_{10}, 14.1 ppm (expt 10.6 ppm) for N_3 (see Figure 6). For the carbon shieldings, the largest change upon reduction is 38.5 ppm (expt 30.4 ppm) for C_{4a}, followed by C_8 with 18.9 ppm (expt 18.5 ppm), C_6 with 21.4 ppm (expt 16.7 ppm), and C_{10a} with 11.2 ppm (expt 12.0 ppm). All other carbon shieldings change by less than 5 ppm. Notably, the order of theoretically predicted oxidized flavin reactivity toward a nucleophile is $N_5 > C_{4a} > C_6 > C_8 > C_{10a}$, although the exact order of C_6 and C_8 reactivity is not consistently predicted.[73,74] In the case of N_1 and N_5, the large change in shielding is undoubtedly due to the change from pyridine to pyrrole-type nitrogen.[51,71] The N_5 center is remarkable for the large paramagnetic component in the oxidized state (144 ppm more deshielded than N_1).

The range of chemical shieldings for pyridine-type nitrogens is quite large, roughly −80 to +175 ppm vs neat nitromethane.[75] Hence, the TARF N_5 shielding, −344.3 ppm vs liquid ammonia or +40 ppm vs nitromethane, is not particularly remarkable (although the pyridine-type nitrogens more deshielded than this are 1,2-diazines). The N_1 shielding however lies at the other end of the pyridine shielding range, −199.9 ppm vs liquid ammonia or +182 ppm vs neat nitromethane. What is most interesting however is the relation between the biological reactivities of these two nitrogens and their shieldings. The two nitrogens have shieldings differing by 146 ppm and are conjugated to one another. The N_5 position has been shown to be the position of biological hydride transfer from NAD(P)H and is also reactive toward sulfite. It is unusually electrophilic for a pyridine-type nitrogen, and this has been supported by numerous ab initio computational studies of the flavin, as mentioned earlier. On the other end of the diazabutadiene moiety is the N_1 nitrogen, which shows the expected pyridine nucleophilic reactivity.[74] In particular, N_1 is the preferred site of protonation of the neutral oxidized flavin, as indicated by ab initio computational studies.

Interaction with cationic protein side chains or protonation at N_1 is expected to increase the reactivity of the N_5 position.[1,23,29,73] Indeed, we report here that protonation of oxidized lumiflavin at N_1 leads to a deshielding of the N_5 GIAO B3PW91//B3PW91 cc-pVTZ resonance from −120.0 to −153.4 ppm, a dramatic 33.4 ppm deshielding (see Table 5). This is due almost exclusively to an increase in the paramagnetic

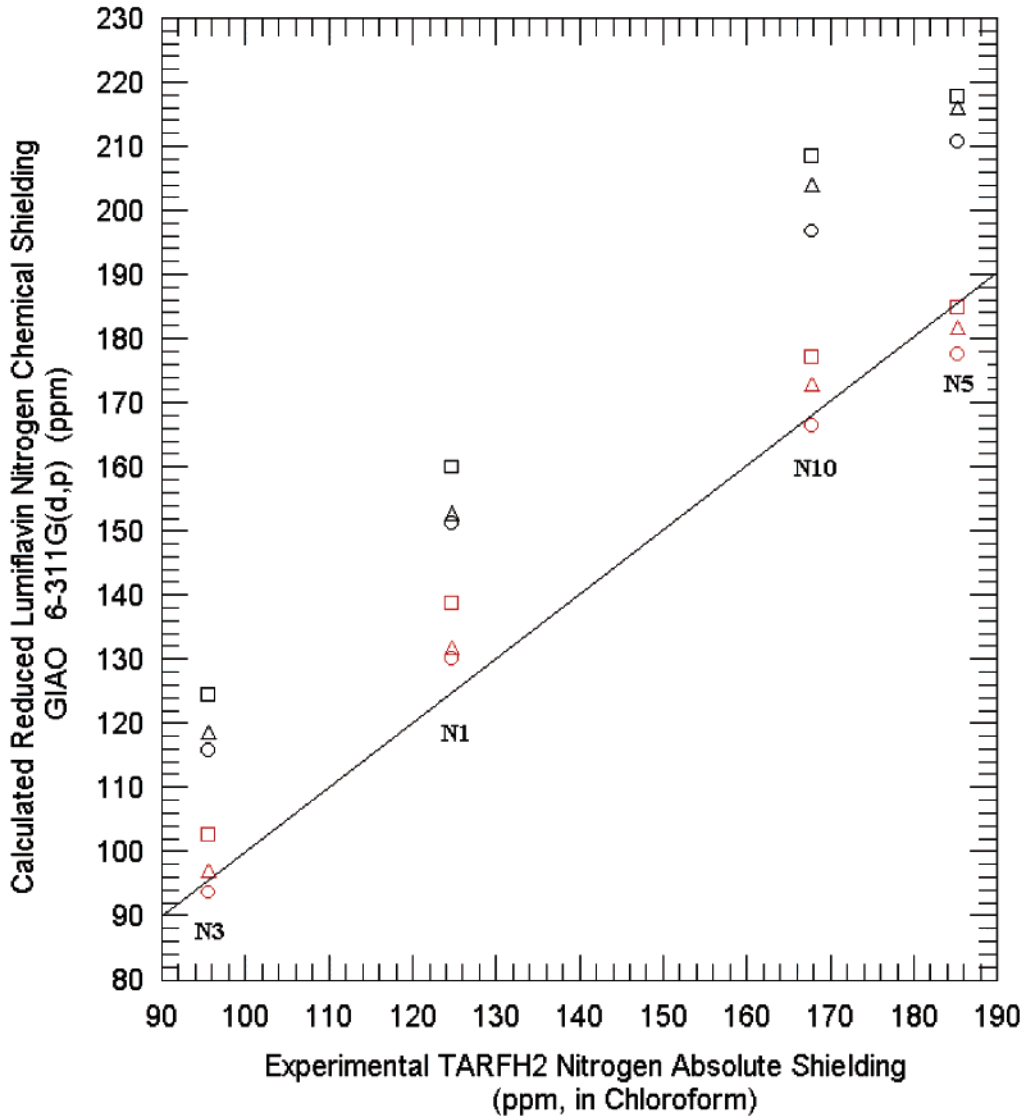

Figure 5. The combined effects of electron correlation (in the geometry and in the shielding calculation) on the NMR shieldings for the nitrogens of reduced flavin. The results compared are as follows: (black □) HF//HF; (black △) HF//B3PW91; (black ○) HF//MP2; (red □) B3PW91//HF; (red △) B3PW91//B3PW91; (red ○) B3PW91//MP2.

TABLE 5: The Flavin N_5 Isotropic Shielding and σ_{11} Principle Value (in parentheses) for the 6-311G(d,p), 6-311G(2d,2p), and cc-pVTZ Basis Sets[a]

	The effect of modification of N_1 on the B3PW91 GIAO NMR shielding (ppm) of the N_5 reactive center		
	N_5 NMR 6-311G(d,p)	N_5 NMR 6-311G(2d,2p)	N_5 NMR cc-pVTZ
Lf_{ox}	−121.4 (−490.5)	−120.7 (−487.1)	−120.0 (−485.5)
Lf_{ox} NH_2CHO	−125.8 (−501.9)	−124.3 (−496.7)	−124.6 (−497.3)
Lf_{ox} $CH_3NH_4^+$	−138.5 (−535.2)	−137.9 (−532.0)	−137.8 (−530.8)
Lf_{ox}^+ (not reopt)	−145.6 (−553.8)	−145.5 (−555.0)	−144.7 (−553.6)
Lf_{ox}^+ (reopt)	−155.0 (−588.1)	−154.5 (−585.5)	−153.4 (−583.5)
1,10-ethylene flavin	−159.6 (−606.4)	−159.0 (−603.7)	−158.0 (−601.5)

[a] The shielding for free oxidized lumiflavin, Lf_{ox}, is given in the first row. In the second and third rows are Lf_{ox} hydrogen bonded at N_1 to an amide group (hydrogen-bonding coordinates taken from flavodoxin of *Clostridium beijerinckii*[34]) and Lf_{ox} with cationic methylamine near the N_1 group (coordinates taken from nitroreductase of *Enterbacter cloacae*[79]). The amide and methylamine groups were optimized with the same basis sets as the corresponding flavin to yield a self-consistent model. In rows four and five are Lf_{ox} protonated at N_1 but not geometry reoptimized and protonated Lf_{ox} that has undergone reoptimization. The last row is the 1,10-ethylene-bridged flavin.[5]

deshielding contribution to the N_5 σ_{11} principle value, by 98.0 ppm. The flavin derivative 1,10-ethylene, which is a good model system for flavoenzyme activation of N_5, showing a dramatic increase in reactivity toward sulfite, likewise shows a deshielding of N_5 by 38.0 ppm.

The dramatic change in the shielding of the σ_{11} principle value is significant because σ_{11} is attributed to $n \rightarrow \pi^*$ transitions in MO theory.[72,76] Indeed, nitrogen shielding principle values are known to be much more sensitive to the molecular environment (in particular hydrogen bonding) of the nitrogen than the

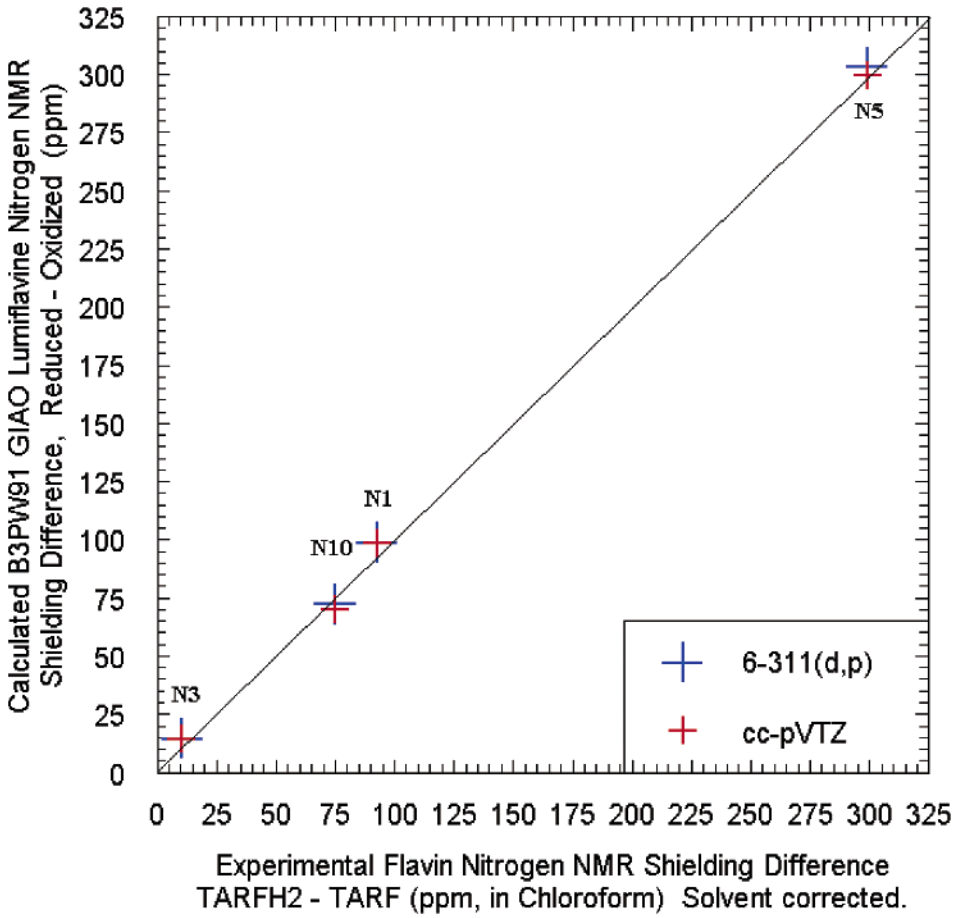

Figure 6. The shielding difference between reduced and oxidized flavin. The N_1 and N_5 experimental shieldings used are the solvent-corrected values.

isotropic value.[77,78] Previously, large changes observed in the σ_{11} of nitrogens in five- and six-membered aromatics upon protonation led to the suggestion that NMR shieldings may be a sensitive measure of intermolecular interactions in biomolecules.[76] Here, we report that even protonation at a distal nitrogen can dramatically influence the in-plane NMR principle value σ_{11}.

The above deshielding at N_5 is partly due to the changes in molecular structure, which result upon formation of a new bond at N_1, and partly because of the positive charge at N_1. Simple protonation of N_1 without reoptimization of the flavin structure does not yield the full effect as is seen by comparing Lf^+ (not reopt) and Lf^+ (reopt) in Table 5. Furthermore, short of protonation, interaction between the N_1 position of the flavin and a cationic amine group results in a 17.2 ppm deshielding at N_5 (44.9 ppm change in σ_{11}). The effect on N_5 shielding of a hydrogen bond at N_1 is only 4.6 ppm (11.8 ppm change in σ_{11}). This supports the notion of a fundamental distinction *in reactivity* between flavoproteins that interact at N_1 with basic side chains and ones that do not, as has been previously suggested.[1] Essentially the same results are obtained with the 6-311G(2d,2p) basis set, and further comparison with the 6-311G(d,p) basis shows that even this much smaller basis gives qualitatively the same results.

Theoretical investigations have consistently predicted nucleophilic reactivity for N_1 due to the large partial negative charge and substantial HOMO density ascribed to this nitrogen.[17,73] Just as the strong degree of shielding at N_1 nitrogen may be related to its nucleophilic reactivity, the results of Table 5 suggest that the degree of deshielding of N_5 may be related to the electrophilic reactivity of that center.

Conclusions

The inclusion of electron correlation in the calculation of NMR shieldings of flavin carbons and nitrogens significantly improves agreement with experiment. Of the two density functional methods considered here, the B3PW91 functional appears to perform somewhat better than the B3LYP functional. In general, inclusion of electron correlation effects appears to lead to *deshielding* of resonances, both directly and due to the effect on geometries. The striking exception is the oxidized flavin N_5 reactive center, which becomes more *shielded* in correlated NMR shieldings than uncorrelated ones (at a fixed geometry). Thus the N_5 resonance comes to within 6.1 ppm of the solvent-corrected experimental value, a dramatic improvement of 60.7 ppm over the uncorrelated result.

For the fully reduced flavin, HF, DFT, and MP2 calculations reveal a correlation between the N_{10} shielding and pyramidalization angle but not the flavin butterfly bend. No correlation is found for N_5. We make two observations about flavin chemical shieldings and reactivity: (i) the flavin centers showing the greatest increase in shielding upon reduction are also the same centers that have been shown experimentally and theoretically to be the most reactive as electrophiles in the oxidized flavin; (ii) perturbations of the flavin at the N_1 position, which are thought to increase the flavin electrophilic reactivity at N_5, result in significant further deshielding of the NMR shielding at N_5.

Acknowledgment. The authors thank Dr. M. Amzel for helpful discussions and suggestions, as well as Dr. M. Meier, Dr. H. Silverstone, and Dr. D. Yarkony. We also thank the

University of Kentucky Computational Science Center for the use of HP X-class and N-class supercomputers, and the office of the vice president for research and graduate studies for a fellowship for J.D.W.

References and Notes

(1) Massey, V.; Hemmerich, P. *Biochem. Soc. Trans.* **1980**, 246−257.
(2) Ghisla, S.; Massey, V. *Eur. J. Biochem.* **1989**, *181*, 1−17.
(3) Fraaije, M. W.; Mattevi *TIBS* **2000**, *25*, 126−132.
(4) Lennon, B. W.; Williams, C. H., Jr.; Ludwig, M. L. *Prot. Sci.* **1999**, *8*, 2366−2379.
(5) Müller, F.; Massey, V. *J. Biol. Chem.* **1968**, *244* (15), 4007−4016.
(6) Müller, F. *Chemistry and Biochemistry of Flavoenzyemes*; CRC Press: Boca Raton, FL, 1991; Vol. 1.
(7) Shinkai, S.; Honda, N.; Ishikawa, Y.; Manabe, O. *Chem. Lett.* **1984**, 327−330.
(8) Shinkai, S.; Honda, N.; Ishikawa, Y.; Manabe, O. *J. Am. Chem. Soc.* **1985**, *107*, 6286.
(9) Decker, K.; Brandsch, R. *Methods of Enyzmology*; Academic Press: New York, 1997; pp 413−423.
(10) Nishimoto, K.; Fukunaga, H.; Yagi, K. *J. Biochem.* **1986**, *100*, 1647−1653.
(11) Cavelier, G.; Amzel, M. L. *Proteins: Struct., Funct., Genet.* **2001**, *43*, 420−432.
(12) Weber, S.; Möbius, K.; Richter, G.; Kay, C. W. M. *J. Am. Chem. Soc.* **2001**, *123*, 3790−3798.
(13) Chateauneuf, G. M.; Brown, R. E.; Brown, B. J. *Int. J. Quantum Chem.* **2001**, *85*, 685−692.
(14) Antony, J.; Medvedev, D. M.; Stuchebrukhov, A. A. *J. Am. Chem. Soc.* **2000**, *122*, 1057−1065.
(15) Hall, L. H.; Orchard, B. J.; Tripathy, S. K. *Int. J. Quantum Chem.* **1987**, *31*, 195−215.
(16) Hall, L. H.; Orchard, B. J.; Tripathy, S. K. *Int. J. Quantum Chem.* **1987**, *31*, 217−242.
(17) Hall, L. H.; Bowers, M. L.; Durfor, C. N. *Biochemistry* **1987**, *26*, 7401−7409.
(18) Vazquez, S. A.; Andrews, S. J.; Murray, C. W.; Amos, R. D.; Handy, N. C. *J. Chem. Soc., Perkin Trans. 2* **1992**, 889−895.
(19) Dixon, D. A.; Lindner, D. L.; Branchaud, B.; Lipscomb, W. N. *Biochemistry* **1979**, *18* (26), 5770−5775.
(20) Teitell, M. F.; Suck, S.-H.; Fox, J. L. *Theor. Chim. Acta* **1981**, *60*, 127−141.
(21) Wouters, J.; Durant, F.; Champagne, B.; Andre, J.-M. *Int. J. Quantum Chem.* **1997**, *64*, 721−733.
(22) Meyer, M.; Hartwig, H.; Schomburg, D. *J. Mol. Struct. (THEOCHEM)* **1996**, *364*, 139−149.
(23) Zheng, Y.-J.; Ornstein, R. L. *J. Am. Chem. Soc.* **1996**, *118*, 9402−9408.
(24) Weber, S.; Richter, G.; Schleicher, E.; Bacher, A.; Möbius, K.; Kay, C. W. M. *Biophys. J.* **2001**, *81*, 1195−1204.
(25) Hasford, J. J.; Rizzo, C. J. *Bioorg. Med. Chem. Lett.* **2002**, *12*, 151−154.
(26) Lee, E.; Medvedev, E. S.; Stuchebrukhov, A. A. *J. Phys. Chem. B* **2000**, *104*, 6894−6902.
(27) Müller, F. CRC Press: Boca Raton, FL, 1991; Vols. 1, 2, and 3.
(28) Moonen, C. T. W.; Vervoort, J.; Müller, F. *Biochemistry* **1984**, *23*, 4859−4867.
(29) Shinkai, S.; Kawanabe, S.; Kawase, A.; Yamaguchi, T.; Manabe, O.; Harada, S.; Nakamura, H.; Kasai, N. *Bull. Chem. Soc. Jpn.* **1988**, *61*, 2095−2102.
(30) Shinkai, S.; Honda, N.; Ishikawa, Y.; Manabe, O. *J. Am. Chem. Soc.* **1989**, *111*, 4928−4935.
(31) Hasford, J. J.; Rizzo, C. J. *J. Am. Chem. Soc.* **1998**, *120*, 2251−2255.
(32) Niemz, A.; Rotello, V. M. *J. Mol. Recognit.* **1996**, *9*, 158−162.
(33) Hasford, J. J.; Kemnitzer, W.; Rizzo, C. J. *J. Org. Chem.* **1997**, *62*, 5244−5245.
(34) Ludwig, M. L.; Pattridge, K. A.; Metzger, A. L.; Dixon, M. M.; Eren, M.; Feng, Y.; Swenson, R. P. *Biochemistry* **1997**, *36*, 1259−1280.
(35) Rüterjans, H.; Fleischmann, G.; Löhr, M.; Knauf, F.; Blümel, M.; Lederer, F.; Mayhew, S. G.; Müller, F. *Biochem. Soc. Tans.* **1996**, *24*, 116−121 and references therein.
(36) Pasquarello, A.; Schlüter, M.; Haddon, R. C. *Phys. Rev. A* **1993**, *47* (3), 1783−1789.
(37) Schulman, J. M.; Disch, R. L. *J. Comput. Chem.* **1998**, *19* (2), 189−194.
(38) Sun, G.; Keretesz, M. *J. Phys. Chem. A* **2000**, *104*, 7398−7403.
(39) Meier, M. S.; Spielmann, H. P.; Bergosh, R. G.; Haddon, R. C., submitted for publication, 2001.
(40) von Rague Schleyer, P.; Maerker, C.; Dransfeld, A.; Jiao, H.; van Eikema, H.; Nicolaas, J. R. *J. Am. Chem. Soc.* **1996**, *118*, 6317−6318.
(41) Kuhn, R.; Boulanger, P. *Ber. Dtsch. Chem. Ges.* **1936**, *B7*, 1557−1566.
(42) Stephens, P. J.; Devlin, F. J.; Chabalowski, C. F.; Frisch, M. J. *J. Phys. Chem.* **1994**, *98* (45), 11623−11627.
(43) Becke, A. D. *J. Chem. Phys.* **1993**, *98*, 5648.
(44) Cheeseman, J. R.; Trucks, G. W.; Keith, T. A.; Frisch, M. J. *J. Chem. Phys.* **1996**, *104* (14), 5497−5509.
(45) van Wüllen, C. *J. Chem. Phys.* **1995**, *102* (7), 2806−2811.
(46) Vignale, G.; Rasolt, M. *Phys. Rev. Lett.* **1987**, *59* (20), 2360−2363.
(47) Frisch, M. J.; Trucks, G. W.; Schlegel, H. B.; Scuseria, G. E.; Robb, M. A.; Cheeseman, J. R.; Zakrzewski, V. G.; Montgomery, J. A., Jr.; Stratmann, R. E.; Burant, J. C.; Dapprich, S.; Millam, J. M.; Daniels, A. D.; Kudin, K. N.; Strain, M. C.; Farkas, O.; Tomasi, J.; Barone, V.; Cossi, M.; Cammi, R.; Mennucci, B.; Pomelli, C.; Adamo, C.; Clifford, S.; Ochterski, J.; Petersson, G. A.; Ayala, P. Y.; Cui, Q.; Morokuma, K.; Malick, D. K.; Rabuck, A. D.; Raghavachari, K.; Foresman, J. B.; Cioslowski, J.; Ortiz, J. V.; Stefanov, B. B.; Liu, G.; Liashenko, A.; Piskorz, P.; Komaromi, I.; Gomperts, R.; Martin, R. L.; Fox, D. J.; Keith, T.; Al-Laham, M. A.; Peng, C. Y.; Nanayakkara, A.; Gonzalez, C.; Challacombe, M.; Gill, P. M. W.; Johnson, B. G.; Chen, W.; Wong, M. W.; Andres, J. L.; Head-Gordon, M.; Replogle, E. S.; Pople, J. A. *Gaussian 98*, revision A.9; Gaussian, Inc.: Pittsburgh, PA, 1998.
(48) Jameson, C. J. *J. Chem. Phys.* **1981**, *74*, 81−88.
(49) Jameson, A. K.; Jameson, C. J. *Chem. Phys. Lett.* **1987**, *134* (5), 461−466.
(50) Jameson, C. J. *Chem. Rev.* **1991**, *91*, 1375−1395.
(51) Witanowski, M.; Sicinska, W.; Biernat, S.; Webb, G. A. *J. Magn. Reson.* **1991**, *91*, 289−300.
(52) Reibenspies, J. H.; Guo, F.; Rizzo, C. J. *Org. Lett.* **2000**, *2* (7), 903−906.
(53) Norrestam, R.; Stensland, B. *Acta Crystallogr.* **1972**, *B28*, 440−447.
(54) Wouters, J.; Evrard, G.; Durant, F. *Acta Crystallogr.* **1995**, *C51*, 1223−1227.
(55) Wouters, J.; Moureau, F.; Perpete, P.; Norberg, B.; Evrard, G.; Durant, F. *J. Chem. Cryst.* **1994**, *24* (9), 607−614.
(56) Tanaka, N.; Ashida, T.; Sasada, Y.; Kakudo, M. *Bull. Chem. Soc. Jpn.* **1969**, *42*, 1546−1554.
(57) Ertan, A.; Koziol, J. *Acta Crystallogr.* **1993**, *C49*, 2179−2181.
(58) Tanaka, N. *Kagaku no Ryoiki* **1972**, *26*, 62−64.
(59) De Dios, A. C.; Jameson, C. J. *Ann. Rep. NMR Spectrosc.* **1999**, *29*, 5−12 and references therein.
(60) Gauss, J. *J. Chem. Phys.* **1993**, *99* (5), 3629−3643.
(61) Koch, R.; Wiedel, B.; Wentrup, C. *J. Chem. Soc., Perkin. Trans. 2* **1997**, 1851−1859.
(62) Norrestam, R.; von Glehn, M. *Acta Crystallogr.* **1972**, *B28*, 434−440.
(63) Werner, P.-E.; Ronnquist, O. *Acta Chem. Scand.* **1970**, *24*, 997−1009.
(64) Werner, P.-E.; Linnros, B.; Leijonmarck, M. *Acta Chem. Scand.* **1971**, *25*, 1297−1312.
(65) Leijonmarck, M.; Werner, P.-E. *Acta Chem. Scand.* **1971**, *25*, 2273−2290.
(66) Porter, D. J. T.; Voet, D. *Acta Crystallogr.* **1978**, *B34*, 2598−2610.
(67) Haddon, R. C.; Scott, L. T. *Pure Appl. Chem.* **1986**, *58* (1), 137−142.
(68) Haddon, R. C. *J. Phys. Chem. A* **2001**, *105*, 4164−4165.
(69) Haddon, R. C. *J. Am. Chem. Soc.* **1990**, *112*, 3385−3389.
(70) Karplus, M.; Das, T. P. *J. Chem. Phys.* **1961**, *34*, 1683−1692.
(71) Karplus, M.; Pople, J. A. *J. Chem. Phys.* **1963**, *38* (12), 2803−2807.
(72) Witanowski, M.; Stefaniak, L.; Webb, G. A. *J. Magn. Reson.* **1981**, *11B*, Tables 1, 2.
(73) Platenkamp, R. J.; Palmer, M. H.; Visser, A. J. W. G. *Eur. Biophys. J.* **1987**, *14*, 393−402.
(74) Sun, M.; Song, P.-S. *Biochemisry* **1973**, *12* (23), 4663−4669.
(75) Witanowski, M.; Stefaniak, L.; Webb, G. A. *J. Magn. Reson.* **1981**, *11B*, 120−122, Table 13.
(76) Solum, M. S.; Altmann, K. L.; Strohmeier, M.; Berges, Y.; Zhang, D. A.; Facelli, J. C.; Pugmire, R. J.; Grant, D. M. *J. Am. Chem. Soc.* **1997**, *119*, 9804−9809.
(77) Facelli, J. C.; Pugmire, R. J.; Grant, D. M. *J. Am. Chem. Soc.* **1996**, *118*, 5488−5489.
(78) Wei, Y.; de Dios, A. C.; McDermott, A. E. *J. Am. Chem. Soc.* **1999**, *121*, 10389−10394.
(79) Haynes, C.; Koder, R.; Miller, A.-F.; Rodgers, D., in press, 2002.